Analysis and Tunable Models for Phosphor-Converted White Light-Emitting Diode Based on Spectral Compensation

Xuehua Shen, Huanting Chen, Wenjie Zhang, Xiaoxi Ji, and Yan Yi

***Abstract*—The correlated color temperature (CCT) and color rendering index (CRI) are two significant indicators related to the color appearance and visual effects of illumination. This paper concentrates on dynamic dimming for phosphor-converted (PC) white LEDs to achieve tunable CCT and adequate CRI, via compensation of red/green spectra. The LED systems described have a simple configuration consisting of a PC white LED, a monochrome green LED and a monochrome red LED, which can be individually driven. Compared to individual PC white LEDs, both the spectral continuity and uniformity of the mixed white light are enhanced. The tunable dimming models are proposed by combination of spectral colorimetry and photo-electro-thermal (PET) theory, thus multi-physics effects are involved. From the modeling process and results, the nonlinear characteristics are observed. Experimental verifications present good agreement existing between calculations and measurements, both in terms of values and variation trends. These proposed models could be effective tools to figure out photometric characteristics and visual perception of illumination. On the other hand, they could provide schemes of reference to improve the illumination environment adapting to various special occasions and personal preferences.**

***Index Terms*—Light-emitting diodes (LED), correlated color temperature (CCT), color rendering index (CRI), spectral compensation, tunable dimming, spectral optimization.**

Manuscript received 15 March 2023; accepted 26 April 2023. Date of publication 1 May 2023; date of current version 12 May 2023. This work was supported in part by the National Natural Science Foundation of China under Grants 62001200 and 61975072, in part by the Natural Science Foundation of Fujian Province under Grants 2020J01817, 2020J01820, and 2021J011009, in part by the Program for Innovative Research Team in Science and Technology in Fujian Province University, Optoelectronic Materials and Device Application, in part by the Industry-University-Research Collaboration Foundation of the Fujian Province under Grant 2020H6017, in part by the Natural Science Foundation of Zhangzhou under Grant ZZ2021J11, in part by the Natural Science Foundation of the Fujian Higher Education Institutions under Grant JAT200316, and in part by the National College Students' Innovation and Entrepreneurship Training Program under Grants 202010402017, 202110402001, 202110402013, and 202110402028X. *(Corresponding authors: Xuehua Shen; Huanting Chen.)*

Xuehua Shen is with the College of International Cruise and Yacht, Guangzhou Maritime University, Guangzhou 510725, China, and also with the Optoelectronic Materials and Device Application Industry Technological Development Base of Fujian Province, Zhangzhou 363000, China (e-mail: fj_sxh39@163.com).

Huanting Chen and Wenjie Zhang are with the College of Physics and Information Engineering, Minnan Normal University, Zhangzhou 363000, China, and also with the Optoelectronic Materials and Device Application Industry Technological Development Base of Fujian Province, Zhangzhou 363000, China (e-mail: htchen23@qq.com; 2534855703@qq.com).

Xiaoxi Ji and Yan Yi are with the College of International Cruise and Yacht, Guangzhou Maritime University, Guangzhou 510725, China (e-mail: jixiaoxi@gzmtu.edu.cn; yiyan@gzmtu.edu.cn).

Digital Object Identifier 10.1109/JPHOT.2023.3272069

I. Introduction

RAPID advancements of light-emitting diode (LED) theories and technologies make LED devices and systems become replacements of traditional light sources such as incandescent and fluorescent lamps [1]. They have been regarded as the fourth-generation lighting sources due to advantages of high luminous efficiency, color-tunable property, and environmental safety [2]. For general lighting, white LEDs can be manufactured by several approaches, among which phosphor-converted (PC) white LEDs integrated of $Y_3Al_5O_{12}$:Ce^{3+}(YAG:Ce^{3+}) phosphors and blue GaN-based chips occupy the market mainstream, owing to technology maturity and economic efficiency [3]. The spectra emitted from PC white LEDs cover most regions of visible light, equipped with a certain extent of spectral continuity. However, what cannot be ignored is that, these PC white LEDs generally have relatively fixed and high correlated color temperature (CCT), and meanwhile suffer from low color rendering index (CRI) due to the lack of red and green spectra [4].

It has been confirmed that, the illumination can seriously affect occupants' brightness perception, subjective impression and work performance, even health condition. The mentioned CCT and CRI are key indicators in determining the color appearance and visual effects of illumination, especially for interior space. How CCT has impacts on psychological aspects and subjective mood of occupants in office and residential spaces has been explored [5], [6]. Higher CCT will offer higher degree of brightness levels, to further improve humans' brightness perception and work performance; on the contrary, lower CCT is preferred in bedrooms and recreational areas to promote relaxation [7]. The CRI, indicates how naturally the colors of objects or their surroundings appear under a particular light source [8]. It is a comparative value between 1 and 100, versus natural light (sunlight) which is defined to have a standard CRI of 100 [9]. In daily areas needing correct color judgment (such as living room, office, etc.), the CRI is generally recommended not less than 80; for occasions with particularly high demands on accurate color contrast (such as museums, art galleries, etc.), the CRI should be above 90 to satisfy illumination criteria [10].

For sophisticated occasions (such as museums, art galleries, exhibition centers, hotels, cruise ship and cabin banquet halls, etc.), dynamic illumination with tunable CCT is an expectation,

while an adequate CRI must be guaranteed, thus to provide a perfect and comfortable visual perception according to specific scenes [11]. However, accurate and dynamic dimming control of CCT is a difficult task for individual PC white LEDs, since their spectral components and proportions are relatively fixed [12], [13]. To achieve tunable CCT, LED systems based on bicolor LED sources are popular configurations, which generally consist of PC white LEDs respectively with a low CCT and a high CCT, allowing the continuous change of CCT from the low value to the high one [14]. Nevertheless, these systems are unable to achieve a great improvement in CRI due to insufficient red/green spectra of PC white LEDs [15]. Tricolor LED systems composed of trichromatic LED chips (i.e., red, green and blue LED chips) can also obtain tunable CCT, via individually controlling monochromatic LEDs to adjust the spectral structure [16]. Regrettably, as the full width at half maximum (FWHM) of each monochromatic spectrum is relatively narrow, it is still not easy to get a high CRI [17]. On the other hand, to achieve white light with high CRI, multi-phosphors-converted LEDs based on blue GaN-based LED chips are alternative to be considered, in which appropriate red/green phosphors should be added together with YAG:Ce^{3+} phosphors [18]. But resulted from a cyan spectral valley within 470–500 nm, a high enough CRI is still a difficult task [19]. Near-ultraviolet LED chips combined with red, green, and blue (RGB) trichromatic phosphors are another option to improve color rendering [20], which are anticipated to yield broad spectra. However, there exists an inescapable problem of low luminous efficacy, hindering their widespread adoption in practice [21]. For above schemes to improve color rendering, as different kinds of phosphors are solidified in epoxy or silicone then coated on the single LED chip, to separately control the emission spectrum converted by a certain kind of phosphors seems impossible, leading to non-tunable CCT. Obviously, it is really a challenge to realize satisfying white light with tunable CCT and high CRI simultaneously.

In view of this, the study in this paper is primarily targeted at effective dimming modeling for the widely used PC white LEDs to achieve tunable CCT and adequate CRI, through compensation of red/green spectra. The LED systems described are respectively consisted of a PC white LED, a monochrome green LED and a monochrome red LED, which can be individually driven. How optical properties of the mixed white light are influenced by superimposing red/green spectra is theoretically analyzed and experimentally discussed. The tunable dimming models are proposed based on the spectral colorimetry and general photo-electro-thermal (PET) theory, therefore somehow taking into account coupling effects of multi-physics fields. Experimental verifications present good agreement existing between calculations and measurements, both in terms of values and variation trends. This kind of LED systems are in simple configurations, maintain advantages of PC white LEDs, while obtain additional capacities including tunableness of CCT and improvement of CRI. It provides schemes of reference to make illuminations adapting to various special occasions and personal preferences. Meanwhile, these models could be feasible tools to fairly figure out photometric characteristics and visual perception of illumination.

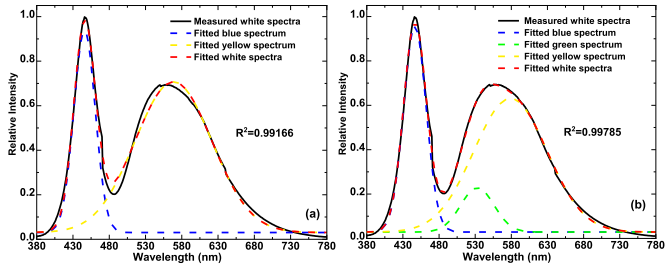

Fig. 1. SPD fitting of PC white LED: (a) bicolor (blue-yellow) Gaussian model. (b) tricolor (blue-yellow-green) Gaussian model.

II. Analysis of PC White LEDs and Spectral Compensation

A. Spectral Characteristics of PC White LEDs

The blue GaN-based LED chips and YAG:Ce^{3+} phosphors are two crucial parts related to spectral characteristics of PC white LEDs. The blue GaN-based LED chips turn most of injection electrical power into blue spectrum accompanied with a fraction of heat dissipation; YAG:Ce^{3+} phosphors then absorb a part of blue spectrum through the allowed $4f^1$-$5d^1$ transition and emit out yellow spectrum via the reverse $5d^1$-$4f^1$ transition [22]. The desired white light is consequently generated by mixture of the remaining transmitted blue spectrum and converted yellow spectrum. However in a strict sense, these YAG:Ce^{3+} phosphors actually emit a mass of yellow spectrum as well as a fraction of green spectrum [23]. It can be certified by the spectral fittings exhibited in Fig. 1, where the spectral power distribution (SPD) of a PC white LED is respectively fitted with the bicolor (blue-yellow) and tricolor (blue-yellow-green) Gaussian models. It is observed that, the fitting degree of tricolor Gaussian model (0.99785) is larger than that of bicolor Gaussian model (0.99166), proving the existence of green spectrum.

For human beings, there are three photoreceptor cells in eyes to have visual perception corresponding to three basic colors respectively of red, green and bule. It could be regarded as the biostructure foundation for spectral colorimetry theory, explaining why different spectra have different visual effects on human beings. According to spectral trichromatic theory, the desired white light can be theoretically obtained by mixture of red, green and blue spectra, and their spectral components will strongly determine optical properties of the mixed white light, including CCT, CRI, chromaticity coordinates, etc. Combining Fig. 1 with trichromatic theory, there is an obvious imperfection of white light emitted from PC white LEDs, i.e., insufficiency of red/green spectra. Actually, this is a crucial causality of the poor color rendering property of individual PC white LEDs.

Within the mixed white light of the three primary colors (RGB) spectra, the green spectrum is particularly important, as it accounts for more than 50% of the brightness and moreover is located at the center within the wavelength range of visible spectroscopy. The red spectrum is also indispensable to obtain satisfying white light, since its insufficiency will directly lead to lower CRI and higher CCT of the mixture spectra. Clearly, for general lighting applications of PC white LEDs, it is necessary

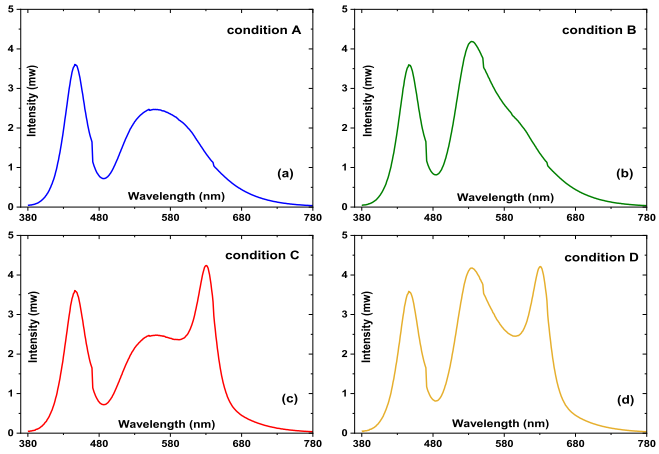

Fig. 2. SPDs of mixed white light: (a) Without spectral compensation. (b) Compensated with green spectrum. (c) Compensated with red spectrum. (d) Compensated with red and green spectra.

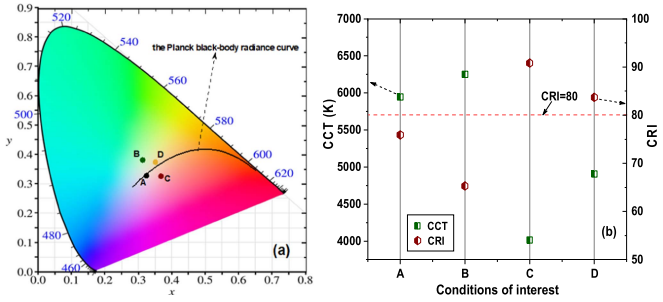

Fig. 3. Chromaticity coordinates, CCT and CRI of mixed white light: (a) Chromaticity coordinates. (b) CCT and CRI.

to compensate extra red/green spectra, so as to improve the illumination quality.

B. Effects of Spectral Compensation on PC White LED

Based on the above analysis, the LED systems we focused are in the simple configuration combining a PC white LED, a monochrome red LED and a monochrome green LED together, which can be individually controlled. In this way, the optical properties of PC white LED will be improved via compensation of red/green spectra. Beforehand, how extra compensated red/green spectra have impacts on the mixed white light has been experimentally analyzed, as shown in Fig. 2. These figures are SPDs respectively of four conditions: an individual PC white LED (condition A), combination of a PC white LED and a monochrome green LED (condition B), combination of a PC white LED and a monochrome red LED (condition C), combination of a PC white LED, a monochrome green LED and a monochrome red LED (condition D). It is observed that, on the basis of individual PC white LED, compensation of both red and green spectra will well enhance the continuity and uniformity of the mixture spectra within the wavelength range of visible spectroscopy.

The corresponding chromaticity coordinates, CCT and CRI of above four conditions are displayed in Fig. 3. It is noticed that, 1) the chromaticity coordinates of emitted light of the individual PC white LED present very close to the Planck black-body radiation curve, somehow signifying that this kind of light sources are really common options to satisfy general lighting; 2) compensation of green spectrum alone will make the chromaticity coordinates drift up to the left, meanwhile the CCT will rise up to a larger value about 6250 K and the CRI is reducing down close to 65; 3) inversely, compensation of red spectrum alone will make the chromaticity coordinates drift to the right and very slightly down, while the CCT will lower down to a smaller value near 4000 K and the CRI is going up to about 91; 4) there is a balance when both red and green spectra are compensated, as condition D, where the chromaticity coordinates move upward and approach the Planck black-body radiation curve, while the CCT drops down to about 4900 K and the CRI is rising up to about 84.

To well restore color features, the CRI is generally required to be higher than 80. As observed from Fig. 3(b), the individual PC white LED has a relatively poor CRI below 80 (almost 75), conditions C and D together indicate that the compensation of red spectrum is necessary to improve color rendering. In conclusion, Figs. 2 and 3 manifest that, compensation of both red and green spectra would potentially achieve tunable CCT as well as adequate CRI, if the compensated spectral components are appropriate and controllable.

III. Tunable Modeling for PC White LEDs With Spectral Compensation

A. Nonlinear CCT Linking Chromaticity Coordinates and Luminous Flux

For a given light source, its chromaticity coordinates, tristimulus values, CCT and luminous flux are interrelated. Refer to colorimetry theory, there are relationships existing between tristimulus values (X, Y, Z) and chromaticity coordinates (x, y, z), expressed as below

$$\begin{cases} x = \frac{X}{X+Y+Z} \\ y = \frac{Y}{X+Y+Z} \\ z = \frac{Z}{X+Y+Z} \end{cases}, \tag{1}$$

Since $x+y+z=1$, it can be derived from (1) that

$$\begin{cases} Y = \frac{y}{x}X \\ Z = \frac{z}{x}X = \frac{1-x-y}{x}X \end{cases}, \tag{2}$$

or

$$\begin{cases} X = \frac{x}{y}Y \\ Z = \frac{z}{y}Y = \frac{1-x-y}{y}Y \end{cases}. \tag{3}$$

Assume that (X_W, Y_W, Z_W) represent tristimulus values of the individual PC white LED, while (X_R, Y_R, Z_R) and (X_G, Y_G, Z_G) denote those respectively of the monochrome red LED and monochrome green LED. Define (X_M, Y_M, Z_M) as tristimulus values of the mixed white light which is the sum of the three LEDs, there are

$$\begin{cases} X_M = X_W + X_R + X_G \\ Y_M = Y_W + Y_R + Y_G \\ Z_M = Z_W + Z_R + Z_G \end{cases}. \tag{4}$$

If (x_W, y_W, z_W), (x_R, y_R, z_R), and (x_G, y_G, z_G) denote chromaticity coordinates respectively of the individual PC white LED, monochrome red LED, and monochrome green LED, then overall chromaticity coordinates of the mixture spectra can be given as, (5) and (6) shown at the bottom of this page.

Since the tristimulus value *Y* represents luminance and generally is proportional to the luminous flux ϕ_v, while chromaticity coordinate *y* can be approximated as in proportion to CCT [24], (6) therefore will be transformed into

$$y_M = \frac{\phi_W + \phi_R + \phi_G}{\frac{\phi_W}{y_W} + \frac{\phi_R}{y_R} + \frac{\phi_G}{y_G}}, \tag{7}$$

where ϕ_W, ϕ_R, and ϕ_G are luminous flux respectively correspond to the individual PC white LED, the monochrome red LED, and the monochrome green LED.

Hence, the CCT of the mixture spectra can be expressed as

$$CCT_M = \eta y_M = \eta \frac{\phi_W + \phi_R + \phi_G}{\frac{\phi_W}{y_W} + \frac{\phi_R}{y_R} + \frac{\phi_G}{y_G}}, \tag{8}$$

where CCT_M is the CCT of the mixture spectra emitted from the LED system, η presents the proportionality coefficient between the mixed CCT_M and chromaticity coordinate y_M, which is related to electrical and thermal characteristics.

Equations (7) and (8) expose the nonlinear characteristics of the mixed y_M and CCT_M, linking up the CCT, luminous flux and chromaticity coordinates of individual LEDs together. They are not only suitable for LED systems combining PC white LED with monochrome red/green LEDs, but also applicable to LED systems integrated by multiple LEDs.

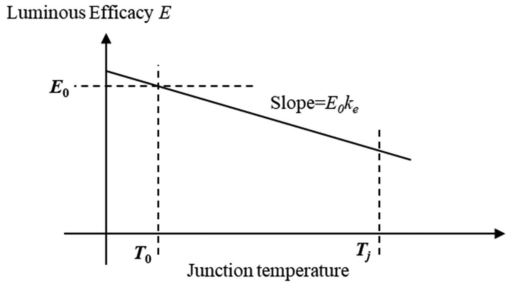

Fig. 4. Typical temperature-dependency of luminous efficacy of LED.

B. Photo-Electro-Thermal Analysis of Luminous Flux

For LED sources, there is a relationship between the luminous flux ϕ_v and injection electric power P_d, that is

$$\phi_v = E \cdot P_d, \tag{9}$$

where *E* is the luminous efficacy (lumen/Watt).

Due to temperature sensitivity of LED sources, the emission intensity would decrease with increasing temperature [25]. This characteristic could be mainly reflected in the temperature-dependency of luminous efficacy *E*, as shown in Fig. 4 (refer to LED manufacturer data sheets).

The temperature-dependency of luminous efficacy in Fig. 4 presents strong linear feature, thus to describe it as

$$E = E_0[1 + k_e(T_j - T_0)], \tag{10}$$

where E_0 denotes the rated luminous efficacy at the rated temperature T_0 (typically 25 °C as given in LED data sheets), T_j is the junction temperature of the LED, and k_e is the relative rate that luminous efficacy reduces with rising temperature.

In practice, heatsink compound or equivalence is generally applied between the LED and heatsink to ensure good thermal contact. In this situation, the thermal property of LED can be

$$\begin{aligned} x_M &= \frac{X_M}{X_M + Y_M + Z_M} \\ &= \frac{X_W + X_R + X_G}{X_W + X_R + X_G + Y_W + Y_R + Y_G + Z_W + Z_R + Z_G} \\ &= \frac{X_W + X_R + X_G}{X_W + X_R + X_G + \frac{y_W}{x_W}X_W + \frac{y_W}{x_R}X_R + \frac{y_G}{x_G}X_G + \frac{1-x_W-y_W}{x_W}X_W + \frac{1-x_R-y_R}{x_R}X_R + \frac{1-x_G-y_G}{x_G}X_G} \\ &= \frac{X_W + X_R + X_G}{\frac{X_W}{x_W} + \frac{X_R}{x_R} + \frac{X_G}{x_G}}, \end{aligned} \tag{5}$$

$$\begin{aligned} y_M &= \frac{Y_M}{X_M + Y_M + Z_M} \\ &= \frac{Y_W + Y_R + Y_G}{X_W + X_R + X_G + Y_W + Y_R + Y_G + Z_W + Z_R + Z_G} \\ &= \frac{Y_W + Y_R + Y_G}{\frac{x_W}{y_W}Y_W + \frac{x_W}{y_R}Y_R + \frac{x_G}{y_G}Y_G + Y_W + Y_R + Y_G\frac{1-x_W-y_W}{y_W}Y_W + \frac{1-x_R-y_R}{y_R}Y_R + \frac{1-x_G-y_G}{y_G}Y_G} \\ &= \frac{Y_W + Y_R + Y_G}{\frac{Y_W}{y_W} + \frac{Y_R}{y_R} + \frac{Y_G}{y_G}}. \end{aligned} \tag{6}$$

described as the simplified steady-state thermal equivalent circuit [26], and the junction temperature T_j thus can be expressed as

$$T_j = T_{hs} + R_{jc}P_{heat} = T_{hs} + R_{jc}k_hP_d, \tag{11}$$

where T_{hs} is the steady-state heatsink temperature, R_{jc} is the junction to case thermal resistance of the LED, and k_h is the heat dissipation coefficient representing the portion of electric power that consumes as heat.

Combine (9)–(11) together, the relationship between luminous flux ϕ_v and electric power P_d can be rewritten as

$$\begin{aligned}\phi_v &= E_0[1 + k_e(T_j - T_0)]P_d \\ &= E_0[1 + k_e(T_{hs} + R_{jc}k_hP_d - T_0)]P_d \\ &= (1 + k_eT_{hs} - k_eT_0)E_0P_d + k_ek_hR_{jc}E_0P_d^2. \end{aligned}\tag{12}$$

Equation (12) indicates that the luminous flux ϕ_v is jointly determined by a series of parameters related to electrothermal characteristics of the LED, such as the electrical power P_d, the steady-state heatsink temperature T_{hs}, the LED's junction to case thermal resistance R_{jc}, coefficients related to thermal properties k_e and k_h. It links up all the photometric, electrical, and thermal aspects of the LED system together.

C. Tunable Dimming Models of Described LED Systems

The artificial lighting has been confirmed to have strong photobiological influences on human beings, of which the blue light hazard (BLH) is one serious issue that has caused for much concern. It refers to the insurgence of potential photochemically induced retinal injury resulting from the radiation exposure within the wavelength range of 400–500 nm [13]. For the LED system described here, the blue spectrum is exactly emitted from the blue GaN-based LED chip within the PC white LED. Avoid to aggravate the degree of BLH, the operation condition of the PC white LED is set fixed, and its corresponding luminous flux ϕ_W and chromaticity coordinate y therefore are constants, respectively denoted as $\phi_{W,0}$ and $y_{W,0}$. In this case, the mixed CCT_M would be regulated via controlling the operation conditions of the monochrome red/green LEDs.

It is clear to observed from (12) that, the function of luminous flux ϕ_v is a parabola of electrical power P_d, i.e., in the form of $\phi_v = \alpha_1P_d + \alpha_2{P_d}^2$. Since electrical power P_d is in proportion to injection current under stable voltage, the relationship between luminous flux ϕ_v and current I_d would be also in a similar form of $\phi_v = \beta_1I_d + \beta_2{I_d}^2$. Hence, the mixed luminous flux ϕ_M (i.e., the sum of luminous flux of individual LEDs) can be expressed as

$$\begin{aligned}\phi_M(I_R, I_G) &= \phi_{W,0} + \phi_R + \phi_G \\ &= \phi_{W,0} + (\beta_{R1}I_R + \beta_{R2}I_R^2) + (\beta_{G1}I_G + \beta_{G2}I_G^2), \end{aligned}\tag{13}$$

where β_{R1} and β_{R2} are coefficients correspond to luminous flux ϕ_R versus current I_R, while β_{G1} and β_{G2} are coefficients correspond to luminous flux ϕ_G versus current I_G.

Though the luminous flux is generally dependent on junction temperature and current intensity. However, if the thermal design of LED system is suitable enough (such as, an excellent heatsink with a small thermal resistance or a temperature-controlled heatsink is adopted to ensure good thermal conduction), the impact of junction temperature will be slight and thus can be neglected [27]. On this occasion, coefficients in (12), i.e., β_{R1}, β_{R2}, β_{G1}, and β_{G2} can be treated as constants.

In preliminary experiments, both monochrome red and green LEDs are tested with changing currents, within current range of 20–180 mA with interval of 20 mA and current range of 50–400 mA with interval of 50 mA. It is observed that, both measured chromaticity coordinates y_R and y_G are basically remained unchanged (within 20–180 mA and 50–400 mA, variations of the red LED are respectively 0.19% and 0.16%, variations of the green LED are respectively 1.80% and 2.53%), thus they can also be treated as constant and respectively denoted as $y_{R,0}$ and $y_{G,0}$. Therefore, the mixed chromaticity coordinate y_M and CCT_M can be reasonably regarded as changing with injection currents of monochrome red/green LEDs, and their expressions respectively corresponding to (7) and (8) are rewritten as

$$\begin{aligned}&y_M(I_R, I_G) \\ &= \frac{\phi_{W,0} + (\beta_{R1}I_R + \beta_{R2}I_R^2) + (\beta_{G1}I_G + \beta_{G2}I_G^2)}{\frac{\phi_{W,0}}{y_{W,0}} + \frac{(\beta_{R1}I_R + \beta_{R2}I_R^2)}{y_{R,0}} + \frac{(\beta_{G1}I_G + \beta_{G2}I_G^2)}{y_{G,0}}}, \end{aligned}\tag{14}$$

$$\begin{aligned}&CCT_M(I_R, I_G) \\ &= \eta\frac{\phi_{W,0} + (\beta_{R1}I_R + \beta_{R2}I_R^2) + (\beta_{G1}I_G + \beta_{G2}I_G^2)}{\frac{\phi_{W,0}}{y_{W,0}} + \frac{(\beta_{R1}I_R + \beta_{R2}I_R^2)}{y_{R,0}} + \frac{(\beta_{G1}I_G + \beta_{G2}I_G^2)}{y_{G,0}}}. \end{aligned}\tag{15}$$

When the current of monochrome green LED is kept as constant $I_{G,0}$, the mixed CCT_M will be expressed as

$$CCT_M(I_R, I_{G,0}) = \eta\frac{\phi_{W,0} + (\beta_{R1}I_R + \beta_{R2}I_R^2) + \phi_{G,0}}{\frac{\phi_{W,0}}{y_{W,0}} + \frac{(\beta_{R1}I_R + \beta_{R2}I_R^2)}{y_{R,0}} + \frac{\phi_{G,0}}{y_{G,0}}}. \tag{16}$$

On the contrary, if the monochrome red LED is operating under constant current $I_{R,0}$, the mixed CCT_M will turn to

$$CCT_M(I_{R,0}, I_G) = \eta\frac{\phi_{W,0} + \phi_{R,0} + (\beta_{G1}I_G + \beta_{G2}I_G^2)}{\frac{\phi_{W,0}}{y_{W,0}} + \frac{\phi_{R,0}}{y_{R,0}} + \frac{(\beta_{G1}I_G + \beta_{G2}I_G^2)}{y_{G,0}}}. \tag{17}$$

While both monochrome red and green LEDs are controlled operating under constant currents respectively of $I_{R,0}$ and $I_{G,0}$, the mixed CCT_M obtained is

$$CCT_M(I_{R,0}, I_{G,0}) = \eta\frac{\phi_{W,0} + \phi_{R,0} + \phi_{G,0}}{\frac{\phi_{W,0}}{y_{W,0}} + \frac{\phi_{R,0}}{y_{R,0}} + \frac{\phi_{G,0}}{y_{G,0}}}. \tag{18}$$

In this way, (15) would probably be transformed into a simple form, i.e., polynomial of variable I_R and polynomial of variable I_G multiply each other, as below

$$\begin{aligned}CCT_M(I_R, I_G) = &\frac{\eta}{\frac{\phi_{W,0} + \phi_{R,0} + \phi_{G,0}}{\frac{\phi_{W,0}}{y_{W,0}} + \frac{\phi_{R,0}}{y_{R,0}} + \frac{\phi_{G,0}}{y_{G,0}}}} \\ &\times \left(\frac{\phi_{W,0} + (\beta_{R1}I_R + \beta_{R2}I_R^2) + \phi_{G,0}}{\frac{\phi_{W,0}}{y_{W,0}} + \frac{(\beta_{R1}I_R + \beta_{R2}I_R^2)}{y_{R,0}} + \frac{\phi_{G,0}}{y_{G,0}}}\right) \end{aligned}$$

$$\times \left(\frac{\phi_{W,0} + \phi_{R,0} + (\beta_{G1} I_G + \beta_{G2} I_G^2)}{\frac{\phi_{W,0}}{y_{W,0}} + \frac{\phi_{R,0}}{y_{R,0}} + \frac{(\beta_{G1} I_G + \beta_{G2} I_G^2)}{y_{G,0}}} \right). \quad (19)$$

According to the above dynamic tunable dimming models as well as their modeling process, several important issues are worth to point out, as following:

1) These models are proposed linking up the spectral colorimetry with general photo-electro-thermal (PET) theory of LED systems, thus have somehow taken into account the coupling effects of multi-physics fields. Their model coefficients are connected with a series of parameters related to structure and properties of LED devices or systems (including heatsink temperature T_{hs}, thermal resistance R_{jc}, heat dissipation coefficient k_h, thermal coefficients k_e, and luminous efficacy E_0, etc.).
2) Though there is not a prediction for CRI, however these dynamic dimming models are proposed direct at the configuration of LED systems which are anticipated to simultaneously achieve tunable CCT and improved CRI. On the basis of widely used PC white LEDs, both monochrome red/green LEDs are incorporated into the system, thus the spectral continuity and uniformity of the mixed white light are enhanced.
3) The nonlinear characteristics could be observed from these dynamic tunable dimming models, indicating that the optical properties of LED systems described are not simply monotonically changing with a certain parameter. Moreover, there might exist a maximum point or optimal point, when aiming at a particular optical property.
4) These tunable dimming models could be effective tools to directly figure out photometric characteristics and visual perception of a given illumination. On the other hand, they could provide schemes of reference to optimize the illumination environment adapting to various special occasions and personal preferences.

IV. Verifications and Discussions

To verify the proposed tunable dimming models of mixed luminous flux ϕ_M, chromaticity coordinate y_M and CCT_M, two LED systems are adopted in experiments and discussed with results. Among them, the system consisting of a PC cool white LED (with a high CCT of 6000 K), a monochrome red LED and a monochrome green LED, is called CW-R-G LED system for short; the other integrated by a PC warm white LED (with a low CCT of 3600 K), a monochrome red LED and a monochrome green LED, is called WW-R-G LED system for short.

In the experimental setup, a Everfine HAAS-2000 spectro-radiometer system with integrating sphere photometer is used for optical measurements, a Peltier-cooled fixture CL-200 is adopted as a temperature-controlled heatsink to ensure good thermal contact of the mounting plate, and two Rigol programmable power supplies are applied to provide stable and adjustable currents for individual LEDs. During optical measurements, the heatsink is controlled at fixed temperature of 25 °C, the current of PC white LED is kept at 300 mA, while currents of monochrome red/green LEDs are respectively adjusted from

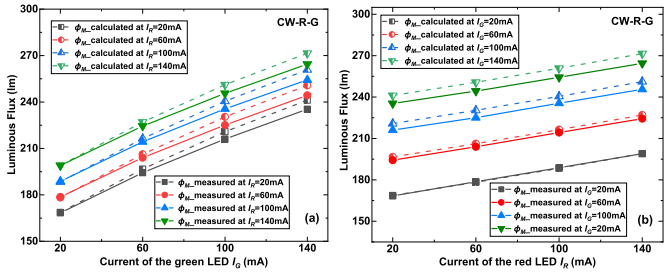

Fig. 5. Calculated and measured luminous flux ϕ_M of CW-R-G LED system: (a) ϕ_M versus current I_G. (b) ϕ_M versus current I_R.

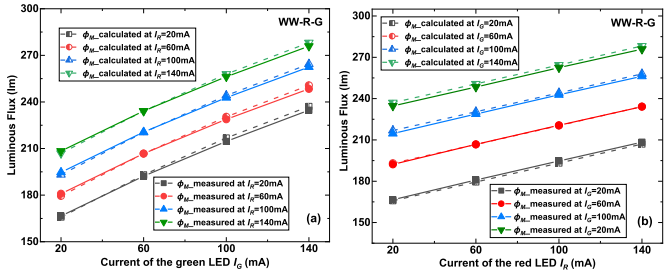

Fig. 6. Calculated and measured luminous flux ϕ_M of WW-R-G LED system: (a) ϕ_M versus current I_G. (b) ϕ_M versus current I_R.

20 mA to 140 mA with interval of 20 mA. All optical measurements are carried out after 20 minutes of steady operation at particular thermal and electrical conditions.

For the convenience of comparison and observation, results of verifications with interval of 40 mA are selected and illustrated in the following figures.

A. The Mixed Luminous Flux ϕ_M and "Efficiency Droop"

The mixed luminous flux ϕ_M calculated from model (13) and their corresponding direct measurements are displayed in Figs. 5 and 6, respectively of the CW-R-G LED system and WW-R-G LED system. As a whole, all calculated results agree quite well with their direct measured values.

By observation, the actual measured values of mixed luminous flux ϕ_M present lower than their calculated ones, and moreover, the difference between them becomes larger when current of green LED I_G increases. As analyzed, it is caused by the "efficiency droop" of the monochrome green LED, which is a common undesirable phenomenon of GaInN/GaN LEDs. The so-called "efficiency droop" means the reduction of internal quantum efficiency (IQE) with increasing current densities [28]. As a controversial topic, several mechanisms have been proposed to explain the origin of this phenomenon, of which Auger recombination and carrier leakage are two most debated and popular ones [29], [30]. The detailed explanation for these two mechanisms is discussed below.

1) Auger Recombination: The IQE of LEDs is generally characterized by the carrier rate equation model with *ABC* coefficients (the *ABC* model) [31]:

$$IQE = \frac{Bn^2}{An + Bn^2 + Cn^3}, \quad (20)$$

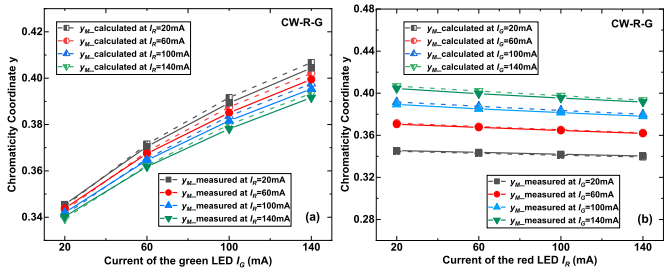

Fig. 7. Calculated and measured chromaticity coordinate y_M of CW-R-G LED system: (a) y_M versus current I_G. (b) y_M versus current I_R.

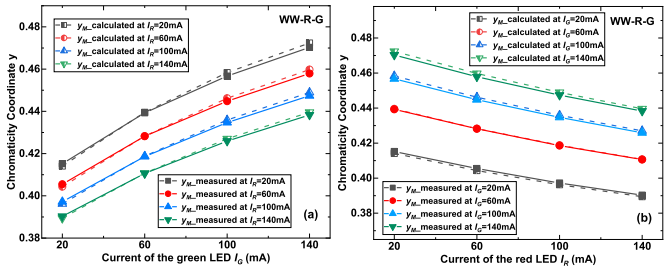

Fig. 8. Calculated and measured chromaticity coordinate y_M of WW-R-G LED system: (a) y_M versus current I_G. (b) y_M versus current I_R.

where n is the carrier density inside the LED; A, B, and C are coefficients which can be extracted by fitting experimental data with the ABC model. Specially, An is the Shockley-Read-Hall recombination rate, Bn^2 is the radiative recombination rate, and Cn^3 is the Auger recombination rate.

Since the Auger recombination rate Cn^3 is proportional to the cube of carrier density n, obviously, it is observed that the IQE would become lower at high carrier/current density, leading to stronger "efficiency droop" [32].

2) Carrier Leakage: Carrier leakage refers to electrons escaping from the active region and recombining with holes in the p-GaN or at the p-contact. Generally, a standard GaN-based LED structure contains an AlGaN electron blocking layer (EBL) at the active region, and the carrier leakage can be suppressed by the conduction band offset between the quantum barrier and quantum well in the active region, as well as between the active region and AlGaN EBL [33]. However, as current density increases, a larger fraction of carriers will have a higher energy, then either the quantum barrier or EBL cannot completely block electrons to escape from the active region [34], finally resulting in enhanced "efficiency droop".

As comparison between Figs. 5 and 6, the "efficiency droop" presents relatively weaker in the WW-R-G LED system than CW-R-G LED system. This difference is mainly related to the impact of "efficiency droop" of blue GaN-based LED on the mixed white light [35]. Specifically, for the PC warm white LED, the blue spectrum emitted from the blue GaN-based LED is a smaller percentage within the white light, when compared to the PC cool white LED [3]. On the basis, if the PC warm white LED and PC cool white LED respectively combine with monochrome red/green LEDs to become the WW-R-G and CW-R-G LED systems, the former will have a much smaller percentage of blue spectrum within the mixed white light, the phenomenon of "efficiency droop" owing to the blue GaN-based LED is therefore relatively weaker [36].

In addition, no matter for the CW-R-G LED system or WW-R-G LED system, the slope of mixed luminous flux ϕ_M versus current I_G is larger than that versus current I_R, confirming that the green spectrum accounts for a great majority of the brightness of the mixed white light.

B. The Mixed Chromaticity Coordinate y_M and CCT_M

According to tunable model (14), the mixed chromaticity coordinate y_M can be predicted with currents, seen from Figs. 7 and 8 respectively of the CW-R-G and WW-R-G LED systems, along with their corresponding measured ones. The agreement between measured and calculated results presents pretty good, both in terms of values and variation trends.

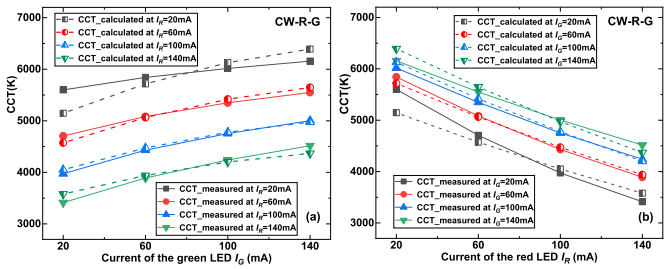

Fig. 9. Calculated and measured of mixed CCT_M of CW-R-G LED system: (a) CCT_M versus current I_G. (b) CCT_M versus current I_R.

Apart from the "efficiency droop" effect explained above, the performance worth mentioning is that, the mixed chromaticity coordinate y_M increases with increasing current I_G at a relative larger slope, but decreases with increasing current I_R relatively slowly. For the CW-R-G LED system, at fixed current I_R of 100 mA, when the current I_G is controlled from 20 mA to 140 mA, the mixed y_M is increasing from 0.3420 to 0.3954, posted a 15.61% growth; at fixed current I_G of 100 mA, when the current I_R is adjusted from 20 mA to 140 mA, the mixed y_M is decreasing from 0.3893 down to 0.3781, posted a 2.87% drop. For the WW-R-G LED system, at fixed current I_R of 100 mA, when the current I_G is controlled from 20 mA to 140 mA, the mixed y_M is changing from 0.3972 to 0.4474, posted a 12.61% growth; at fixed current I_G of 100 mA, when the current I_R is adjusted from 20 mA to 140 mA, the mixed y_M is decreasing from 0.4567 down to 0.4259, posted a 6.74% drop.

Calculations and measurements of mixed CCT_M are displayed in Figs. 9 and 10, respectively of the CW-R-G and WW-R-G LED systems. For the CW-R-G LED system, when it operates at current I_R of 140 mA and current I_G of 20 mA, its mixed CCT_M is 3413 K; if the current I_R is adjusted to 20 mA and the current I_G is adjusted to 140 mA, the mixed CCT_M is increasing to 6157 K. That is, its tunable range is 3413–6157 K. For the WW-R-G LED system, when it operates at current I_R of 140 mA and current I_G of 20 mA, its mixed CCT_M is 2343 K; if current I_R is adjusted to 20 mA and current I_G is adjusted to 140 mA, the mixed CCT_M is increasing to 4799 K. Hence, the corresponding tunable range is 2343–4799 K. Actually, these tunable ranges

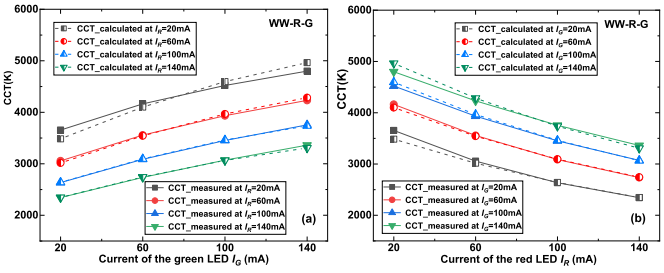

Fig. 10. Calculated and measured of mixed CCT_M of WW-R-G LED system: (a) CCT_M versus current I_G. (b) CCT_M versus current I_R.

TABLE I
ERRORS OF CW-R-G LED SYSTEM

	Root Mean Squared Error	Maximum Relative Error	Mean Relative Error
ϕ_M	4.23 lm	2.69 %	1.53 %
y_M	0.00169	0.67 %	0.39 %
CCT_M	121 K	8.09 %	1.78 %

TABLE II
ERRORS OF WW-R-G LED SYSTEM

	Root Mean Squared Error	Maximum Relative Error	Mean Relative Error
ϕ_M	1.58 lm	1.28 %	0.61 %
y_M	0.00121	0.47 %	0.24 %
CCT_M	55 K	4.69 %	0.93 %

of CCT could well satisfy most daily illumination requirements. Only for occasions with high requirement in illuminance, CCT above 5300 K is necessary. Expect that, the satisfying CCT of general lighting is generally within the range of 2300–5300 K.

As model of mixed CCT_M corresponding to either (15) or (19) is not a simple linear combination of polynomials, the nonlinearity makes the calculations present relatively poor performance at some certain conditions with weaker intensity of current I_R. However, as a whole, the agreement between calculated and measured results is reasonably good.

The root mean squared error, maximum relative error, and mean relative error, respectively of, mixed luminous flux ϕ_M, chromaticity coordinate y_M and CCT_M, are calculated and displayed in Tables I and II respectively correspond to the CW-R-G LED system and WW-R-G LED system. All these errors are within acceptable ranges, providing quantitative supplements to strongly support for the above theoretical derivation and graphics interpretation.

C. The Mixed CRI and Discussion of Improvement

For a light source, its CRI is mainly determined by its spectral structure. The more similar the SPD of a light source is to the natural light, the higher CRI it obtains, and the reverse is also true [37]. Though, both CRI and CCT are related to the spectral structure, they are two independent parameters to describe the optical performance of a light source [38]. The LED systems studied are realized by combination of PC white LEDs and

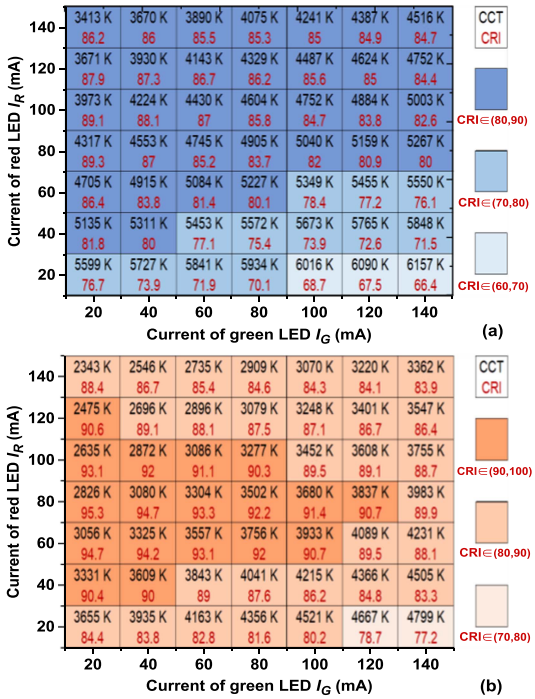

Fig. 11. CRI and CCT of mixed white light versus currents I_R and I_G: (a) CW-R-G LED system. (b) WW-R-G LED system.

monochrome red/green LEDs. Hence compared to individual PC white LEDs, both the spectral continuity and uniformity of the mixed white light are enhanced. Obviously on this occasion, as compensated by red/green spectra, both the CCT and CRI of the mixed white light would be changing due to the variation in SPD [39].

Here, how the compensation of red/green spectra has impact on CRI is also discussed, as demonstrated in Fig. 11, where values of the mixed CCT are given for ease of analysis.

For the CW-R-G LED system, it could be observed and summarized that, 1) the stronger green spectrum compensated, the lower CRI it presents; 2) as the compensated red spectrum enhances, the CRI firstly increases and then decreases relatively slowly; 3) to obtain CRI above 80, necessary amount of compensated red spectrum is required, thus the current of I_R is suggested preferably controlled above 60 mA; 4) the tunable range of CCT is 3413–5311 K, under the satisfying demand that the CRI is higher than 80.

For the WW-R-G LED system, it could be observed and summarized that, 1) similarly, its CRI monotonically decreases with intensity of compensated green spectrum; 2) as the compensated red spectrum enhances, the CRI also increases at first and then decreases, however its values basically above 80, even as high as 95.3; 3) only when a large quantity of green spectrum but a small quantity of red spectrum are compensated (such as conditions that current I_R is not higher than 20 mA while current I_G varies within 120–140 mA), the CRI is slightly lower than 80; 4) the corresponding tunable range of CCT is 2343–4521 K, under the satisfying demand that the CRI is higher than 80.

It is worth mentioning that, for the PC cool white LED without spectral compensation, the CRI is 75.9; when it combines with

the monochrome red/green LEDs to become the CW-R-G system, the CRI can be improved as high as 89.3, the maximum rate of improvement is 17.65%. For the PC warm white LED without spectral compensation, the CRI is 77.8; when it combines with the monochrome red/green LEDs to become the WW-R-G system, the CRI can be improved up to 95.3, the maximum rate of improvement is 22.49%.

For comparison, we have carried out a series of experiments using a dual PC white LED system manufactured by CREE. It is integrated by two PC white LEDs respectively with high CCT of 7600 K and low CCT of 2700 K. When individually tested, the CRI of the LED with high CCT is 79.6, while the CRI of the LED with low CCT is 82.3. When they are integrated together to become the dual PC white LED system, the CRI is ranging from 79.8 to 84.4 under different current conditions, the maximum rate of improvement is 6.03%. In the experiments, the dual PC white LEDs are placed on the Peltier-cooled fixture CL-200 at fixed temperature of 25 °C, and their currents are respectively adjusted from 20 mA to 200 mA with interval of 20 mA.

Obviously from above, our proposed LED systems integrated by PC white LED and monochrome red/green LEDs could obtain a CRI improved with a relatively larger amplitude when compared with the dual PC white LED system.

D. Brief Description on Temperature/Current Dependency

The thermal sensitivity is a common issue for semiconductor devices [40]. For most LED devices and systems, under a poor heat dissipation condition, the increasing temperature could result in change of spectral structure and color feature [33]. On the other hand, as electroluminescence devices, LEDs' optical properties are closely associated with injection currents [41]. Different current intensities mean different injection electric power, and the internal heat generation and accumulation under a fixed heat dissipation condition is also different. Therefore, the spectral intensity and structure, as well as the color feature would be changing with current [42].

As our manuscript mainly concentrates on discussing how compensation of red/green spectra has impact on individual PC-white LEDs, and moreover a Peltier-cooled fixture CL-200 is adopted as a temperature-controlled heatsink to ensure good thermal contact, thus the heat dissipation condition is regarded as adequate enough and the temperature dependency has not been experimental discussed here.

V. Conclusion

Dynamic illumination with tunable CCT and adequate CRI is an expectation, thus to achieve a comfortable visual perception and meanwhile to truthfully present color features of objects. In this paper, the dynamic tunable dimming models are proposed for the widely used PC white LEDs, by combining the monochrome red/green LEDs. With compensation of red/green spectra, both the spectral continuity and spectral uniformity of the mixed white light are enhanced. The described LED systems are in a simple configuration, they maintain advantages of PC white LEDs while obtain additional capacities including tunableness of CCT and improvement of CRI. As these tunable dimming models are proposed by combination of spectral colorimetry and photo-electro-thermal (PET) theory, multi-physics effects are taking into account, the model coefficients therefore are related to a series of parameters in connection with multi-physics properties of LED devices or systems.

The feasibility and usefulness of this kind of LED systems as well as the proposed tunable dimming models are confirmed with experiments, where good agreement between calculated and measured results is obtained. By comparison with the dual PC white LED system, it is indicated that the proposed LED systems integrated by PC white LED and monochrome red/green LEDs could obtain a CRI improved with a relatively larger amplitude.

The study in this paper provides references for design and optimization of illumination adapting to special occasions and personal preferences, and also offers effective tools to figure out the corresponding photometric characteristics and visual perception.

References

[1] S. Y. Hui, A. T. L. Lee, and S. C. Tan, "New dynamic photo-electro-thermal modeling of light-emitting diodes with phosphor coating as light converter part I: Theory, analysis, and modeling," *IEEE Trans. Emerg. Sel. Topics Power Electron.*, vol. 8, no. 1, pp. 771–779, Mar. 2020.

[2] L. X. Nian, X. M. Pei, Z. L. Zhao, and X. Z. Wang, "Review of optical designs for light-emitting diode packaging," *IEEE Trans. Compon. Packag. Manuf. Technol.*, vol. 9, no. 4, pp. 642–648, Apr. 2019.

[3] H. Y. Peng and F. K. Yam, "Comparison of the changes in luminescence properties between cool white and warm white leds at varying temperatures," *IEEE Trans. Compon. Packag. Manuf. Technol.*, vol. 8, no. 12, pp. 2113–2121, Dec. 2018.

[4] A. Wang et al., "White light-emitting diodes with ultrahigh color rendering index by red/green phosphor layer configuration structure," *IEEE Trans. Electron Devices*, vol. 66, no. 12, pp. 5209–5214, Dec. 2019.

[5] J. Nie et al., "Optimization of the dynamic light source considering human age effect on visual and non-visual performances," *Opt. Laser Technol.*, vol. 145, 2022, Art. no. 107463.

[6] J. Toftum, A. Thorseth, J. Markvart, and Á. Logadóttir, "Occupant response to different correlated colour temperatures of white LED lighting," *Build. Environ.*, vol. 143, pp. 258–268, Jul. 2018.

[7] K. C. H. J. Smolders and Y. A. W. Kort, "Investigating daytime effects of correlated colour temperature on experiences, performance, and arousal," *J. Environ. Psychol.*, vol. 50, pp. 80–93, Jun. 2017.

[8] J. H. Oh, S. J. Yang, and Y. R. Do, "Healthy, natural, efficient and tunable lighting: Four-package white LEDs for optimizing the circadian effect, color quality and vision performance," *Light: Sci. Appl.*, vol. 3, no. 2, Feb. 2014, Art. no. e141.

[9] T. E. Houser, M. P. Royer, and J. Christoffersen, "A method and tool to determine the colorimetric and photobiological properties of light transmitted through glass and other optical materials," *Build. Environ.*, vol. 215, no. 1, May 2022, Art. no. 108957.

[10] R. Dang, N. Wang, G. Liu, Y. Yuan, J. Liu, and H. J. Tan, "Illumination in museums: Four-primary white LEDs to optimize the protective effect and color quality," *IEEE Photon. J.*, vol. 11, no. 1, Feb. 2019, Art. no. 8200315.

[11] J. Y. Ding et al., "A novel broad-band cyan light-emitting oxynitride based phosphor used for realizing the full-visible-spectrum lighting of WLEDs," *J. Lumin.*, vol. 231, Mar. 2021, Art. no. 117786.

[12] H. Wang, Y. Mou, Z. Lei, Q. Wang, Y. Peng, and M. Chen, "Enhanced color quality of phosphor-converted white laser diodes through bicolor phosphor-in-glass," *IEEE Trans. Electron Devices*, vol. 68, no. 11, pp. 5652–5655, Nov. 2021.

[13] H. T. Zhu, R. L. Fu, Y. H. Shi, Q. J. He, H. Wang, and X. H. Liu, "Multi-colour light emission based on pixel-array phosphor layer in LEDs," *J. Lumin.*, vol. 221, May 2020, Art. no. 117057.

[14] H. T. Chen, S. C. Tan, and S. Y. Hui, "Nonlinear dimming and correlated color temperature control of bicolor white LED systems," *IEEE Trans. Power Electron.*, vol. 30, no. 12, pp. 6934–6947, Dec. 2015.

[15] G. He and J. Tang, "Spectral optimization of phosphor-coated white LEDs for color rendering and luminous efficacy," *IEEE Photon. Technol. Lett.*, vol. 26, no. 14, pp. 1450–1453, Jul. 2014.

[16] X. Q. Zhan, W. G. Wang, and H. S.-H. Chung, "A novel color control method for multi-color LED systems to achieve high color rendering indexes," *IEEE Trans. Power Electron.*, vol. 33, no. 10, pp. 8246–8258, Oct. 2018.

[17] Q. Yao, L. T. Zhang, Q. Dai, and J. Uttley, "Quantification of trichromatic light sources to achieve tunable photopic and mesopic luminous efficacy of radiation," *J. Illum. Eng. Soc.*, vol. 15, no. 4, pp. 271–280, Jan. 2019.

[18] A. Wang et al., "White light-emitting diodes with ultrahigh color rendering index by red/green phosphor layer configuration structure," *IEEE Trans. Electron Devices*, vol. 66, no. 12, pp. 5209–5214, Dec. 2019.

[19] M. Zhao et al., "Emerging ultra-narrow-band cyan-emitting phosphor for white LEDs with enhanced color rendition," *Light, Sci. Appl.*, vol. 8, no. 1, Apr. 2019, Art. no. 38.

[20] X. Y. Huang, S. Y. Wang, B. Li, Q. Sun, and H. Guo, "High-brightness and high-color purity red-emitting $Ca_3Lu(AlO)_3(BO_3)4:Eu^{3+}$ phosphors with internal quantum efficiency close to unity for near-ultraviolet-based white-light-emitting diodes," *Opt. Lett.*, vol. 43, no. 6, pp. 1307–1310, Mar. 2018.

[21] H. Wang et al., "Phosphor glass-coated sapphire with moth-eye microstructures for ultraviolet-excited white light-emitting diodes," *IEEE Trans. Electron Devices*, vol. 66, no. 7, pp. 3007–3011, Jul. 2019.

[22] A. J. Huang, K. K. Pukhov, K. L. Wong, and P. A. Tanner, "Temperature dependence of the local field effect in YAG:Ce^{3+}nanocomposites," *Nanoscale*, vol. 13, no. 22, pp. 10002–10009, Jun. 2021.

[23] H. T. Chen and S. Y. Hui, "Dynamic prediction of correlated color temperature and color rendering index of phosphor-coated white light-emitting diodes," *IEEE Trans. Ind. Electron.*, vol. 61, no. 2, pp. 784–797, Feb. 2014.

[24] X. H. Shen, H. T. Chen, W. R. Shi, and Q. Y. Xiong, "Electrical and thermal effects of tunable LED systems on lighting and non-visual biological characteristics," *IEEE Photon. J.*, vol. 12, no. 3, Jun. 2020, Art. no. 8200313.

[25] Z. Peng et al., "Temperature-dependent carrier recombination and efficiency droop of AlGaN deep ultraviolet light-emitting diodes," *IEEE Photon. J.*, vol. 12, no. 1, Feb. 2020, Art. no. 8200108.

[26] S. Y. Hui and Y. X. Qin, "A general photo-electro-thermal theory for light emitting diode (LED) systems," *IEEE Trans. Power Electron.*, vol. 24, no. 8, pp. 1967–1976, Aug. 2009.

[27] H. T. Chen et al., "Flicker modeling of white light emitting diode with sinusoidal waveform," *IEEE Trans. Electron Devices*, vol. 69, no. 12, pp. 6851–6858, Dec. 2022.

[28] H. Jeong, G. H. Cho, and M. S. Jeong, "Redistribution of carrier localization in InGaN-based light-emitting diodes for alleviating efficiency droop," *J. Lumin.*, vol. 242, Dec. 2022, Art. no. 119277.

[29] G. B. Lin et al., "Analytic model for the efficiency droop in semiconductors with asymmetric carrier-transport properties based on drift-induced reduction of injection efficiency," *Appl. Phys. Lett.*, vol. 100, no. 16, Apr. 2012, Art. no. 161106.

[30] J. Iveland, L. Martinelli, J. Peretti, J. S. Speck, and C. Weisbuch, "Direct measurement of auger electrons emitted from a semiconductor light-emitting diode under electrical injection: Identification of the dominant mechanism for efficiency droop," *Phys. Rev. Lett.*, vol. 110, no. 17, Apr. 2013, Art. no. 177406.

[31] A. David and M. J. Grundmann, "Droop in InGaN light-emitting diodes: A differential carrier lifetime analysis," *Appl. Phys. Lett.*, vol. 96, 2010, Art. no. 103504.

[32] A. Herzog, M. Wagner, and T. Q. Khanh, "Efficiency droop in green InGaN/GaN light emitting diodes: Degradation mechanisms and initial characteristics," *Microelectron. Reliab.*, vol. 112, 2020, Art. no. 113792.

[33] C. Y. Jia, C. G. He, and Q. Wang, "Performance improvement of InGaN leds by using strain compensated last quantum barrier and electron blocking layer," *Optik*, vol. 248, 2021, Art. no. 168216.

[34] C. Frankerl et al., "Origin of carrier localization in AlGaN-based quantum well structures and implications for efficiency droop," *Appl. Phys. Lett.*, vol. 117, no. 10, Sep. 2020, Art. no. 102107.

[35] J. Cho, E. F. Schubert, and J. K. Kim, "Efficiency droop in light-emitting diodes: Challenges and countermeasures," *Laser Photon. Rev.*, vol. 7, no. 3, pp. 408–421, 2013.

[36] Y.-C. Tsai, J.-P. Leburton, and C. Bayram, "Quenching of the efficiency droop in cubic phase InGaAlN light-emitting diodes," *IEEE Trans. Electron Devices*, vol. 69, no. 6, pp. 3240–3245, Jun. 2022.

[37] K. A. G. Smet, A. David, and L. Whitehead, "Why color space uniformity and sample set spectral uniformity are essential for color rendering measures," *J. Illum. Eng. Soc.*, vol. 12, no. 1-2, pp. 39–50, Oct. 2015.

[38] Z. Ajrina, R. A. M. Revantino, and F. X. N. Soelami, "Spectral reflectance and chromaticity differences of various colors of interior finishing material samples under tunable LED lamps," *J. Build. Eng.*, vol. 44, 2021, Art. no. 103280.

[39] Y. F. Zhao, P. Zhong, and G. X. He, "Optimization of the light-emitting diode daylight simulator based on the CIE metamerism index method," *Color Res. Appl.*, vol. 47, no. 1, pp. 65–73, May 2021.

[40] K. Kamide, T. Mochizuki, H. Akiyama, and H. Takato, "Effects of the non-radiative recombination and bandgap reduction in heat-recovery solar cell," in *Proc. IEEE 47th Photovolt. Specialists Conf.*, Calgary, AB, Canada, 2020, pp. 2175–2177.

[41] S. Li et al., "Active thermal management of high-power LED through chip on thermoelectric cooler," *IEEE Trans. Electron Devices*, vol. 68, no. 4, pp. 1753–1756, Apr. 2021.

[42] C.-P. Wang, S.-W. Kang, K.-M. Lin, T.-T. Chen, H.-K. Fu, and P.-T. Chou, "Analysis of thermal resistance characteristics of power LED module," *IEEE Trans. Electron Devices*, vol. 61, no. 1, pp. 105–109, Jan. 2014.